Journal of Thermal Science Vol.30, No.6 (2021) 2164–2177

https://doi.org/10.1007/s11630-021-1443-2 **Article ID: 1003-2169(2021)06-2164-14**

Influences of Lateral Double-Layered Deflectors on Cooling Performance of Air-Cooled Condenser

HUANG Wenhui, HUANG Xianwei, YANG Lijun*, DU Xiaoze

Key Laboratory of Power Station Energy Transfer Conversion and System of Ministry of Education, School of Energy Power and Mechanical Engineering, North China Electric Power University, Beijing 102206, China

Abstract: The cooling performance of air-cooled condenser (ACC) is susceptible to adverse impacts of ambient winds. In this work, three kinds of lateral double-layered deflectors installed under the ACC platform are proposed to weaken the unfavorable effects of cross winds. Through CFD simulation methods, the main parameters of thermo-flow performances of a 2×660 MW direct dry cooling system are obtained, by which it can be concluded that the deflectors can effectively reduce the inlet air temperatures while enhance the mass flow rates of upwind fans due to the guiding effect, especially at high wind speeds, while the improvement of cooling capacity of ACCs in the 0° wind direction is weak. The inclined-vertical deflectors are superior to others in performance improvement of ACCs for all cases, which can reduce the turbine back pressure by 12.15% when the wind speed is 12 m/s, so they can be applied to the performance enhancement of ACCs under windy conditions in practical engineering.

Keywords: air-cooled condenser, lateral double-layered deflectors, cooling capacity, turbine back pressure, wind speed and direction

1. Introduction

Traditional coal-fired power plants use a large amount of circulating water to cool exhaust steam, which has caused severe challenge of water resource shortage to their rapid development in arid regions, so direct dry cooling technology comes into being and has been widely accepted thanks to its outstanding water-saving benefit in recent years [1]. Air-cooled condenser (ACC) is the key component of direct dry cooling system, in which the cooling air driven by the large-scale axial flow fans flows through the "A" type flat finned tube bundles to take away the exhausted steam heat from turbine.

The researches on the ambient wind effects have been carried out in the past decades since ambient wind plays key roles in the thermo-flow characteristics of ACCs. Duvenhage and Kröger [2] pointed out that the performance attenuation of ACCs under wind conditions is mainly due to two reasons. One is that the air flow rates of upstream fans are remarkably reduced, and the other is that the hot plume recirculation of both banks in the downstream ACCs becomes serious. Rooyen and Kröger [3] concluded through numerical simulations that the fan performance degradation rather than hot plume recirculation leads to the performance deterioration of ACCs significantly. Owen and Kröger [4] used experimental and numerical methods to clarify the changes of fan inlet temperature and ACC heat rejection with the atmospheric temperature. Gu et al. [5, 6] discussed the wind effects on ACCs by wind tunnel test,

Received: Sep 18, 2019 AE: TANG Guihua Corresponding author: YANG Lijun E-mail: yanglj@ncepu.edu.cn

Nomenclature

e	exponent of wind speed formula	u	velocity/m·s^{-1}
f_n	polynomial coefficient of the fan pressure drop equation	u_j	velocity component/m·s^{-1}
g_n	polynomial coefficient for the fan tangential velocity	z	vertical distance to the ground/m
h	convection heat transfer coefficient/W·m^{-2}·K^{-1}	**Greek symbols**	
h'	empirical convection heat transfer coefficient/W·m^{-2}·K^{-1}	Γ	diffusion coefficient/m^2·s^{-1}
h_n	polynomial coefficient for convection heat transfer coefficient	ρ	density/kg·m^{-3}
h_s	exhaust steam enthalpy/J·kg^{-1}	Φ	heat rejection/W
h_{wa}	condensate water enthalpy/J·kg^{-1}	φ	variable
k_L	the loss coefficient of flow	**Subscripts**	
L	the finned tube bundles' thickness/m	2	outlet
m	mass flow rate/kg·s^{-1}	a	air
N	number	B	back
p	pressure/Pa	d	deflector
Q	heat transfer rate/kW	f	axial flow fan
q	heat flux/W·m^{-2}	o	original
R_p	ratio of back pressure reduction	θ	peripheral direction
r_n	polynomial factor for pressure loss coefficient	ref	reference
S	source term in governing equations	s	steam
t	temperature/K	wa	water

which is regarded as a necessary and helpful measure for designing direct dry cooling system. Meyer [7] found that the beneficial effects of walkway on the fans are more pronounced in the air-cooled condenser with two banks. Hotchkiss et al. [8] proposed two parameters affecting the fan performance through the study of the impact of off-axis inflow. Liu et al. [9] found that the increased rotational speed of peripheral fans or height of the wind-wall can effectively restrain hot air recirculation, which is mainly dominated by the wind speed and direction. Bredell et al. [10] compared the performance of axial flow fan with different hub-tip-ratios by numerical simulation, and found that the fan with a larger hub-tip-ratio performs better. In addition, the walkway can improve the performance of peripheral fans. Duvenhage et al. [11] investigated the changes of fan performance with the ACC platform height, and obtained a critical value for optimal performance of fans. Yang et al. [12, 13] pointed out that the ambient wind has a greater impact on ACCs at the upwind side and the reversed flow deteriorates the air cooling capacity of upwind cells. In the wind direction of 90°, the air flow rate decrease rather than hot plume recirculation results in a significant degradation of the thermo-flow performance, while the wind direction of 0° is exactly the opposite.

To overcome the adverse effects of cross winds, many studies have focused on the improvement measures. Besides the novel layouts of ACCs [14, 15], spray humidification and installation of additional structures for improving the cooling efficiency are commonly adopted. For the spray humidification, it can effectively reduce the inlet air temperature [16] and improve the cooling performance of ACC [16]. Compared with the spray humidification, additional structural installations attract more attentions due to no consumption of water. Yang et al. [18] found that wider walkway or higher wind-break wall is beneficial to the operation of ACCs under windy conditions. Owen and Kröger [19] studied a cross-type screen installed under the ACC platform and proposed a modified screen configuration to improve the performance of upstream fans and cause little impact on downstream ones. Zhang et al. [20, 21] proposed two effective measures, the windbreak mesh and diffuser orifice plate, to enhance the cooling capacity of ACCs in the presence of winds. A roof windbreak system is proposed by Gu et al. [22] and the best combination of parameters is obtained. Yang et al. [23] analyzed the effects of windscreen extension, flow guiding device and axial flow fan regulation, and found that the performance of ACCs can be improved and the turbine back pressure is reduced. Gao et al. [24] studied the effects of the deflectors installed under the ACC platform and considered that 45° inclination angle is optimal. Huang et al. [25] investigated the effects of various parameters of air deflectors on ACC performance, with wider and more

air deflectors, moderate pitch and 45° inclination recommended.

As an effective measure, the air deflectors in a longitudinal multi-layered form have been thoroughly investigated, while lateral multi-layered deflectors are rarely involved. It is known that the longitudinal deflectors may cause ACC performance degradation under windless condition, and affect the flow and thermal characteristics of the condenser cells behind the deflectors in the presence of winds. In this work, three types of lateral double-layered deflectors are proposed and investigated by CFD simulations, and their effects on the cooling capacity of ACCs under different meteorological conditions are obtained.

2. Models and Approaches

2.1 Physical models

The layout of main buildings and direct dry cooling system of a 2×660 MW power plant is schematically shown in Fig. 1(a), based on the arrangement and structural dimensions of practical engineering. Five typical wind directions are selected to investigate the wind influence upon the performance of ACCs comprehensively. The turbine house, boiler house, chimney and reinforced concrete support columns are all taken into account. Fig. 1(b) displays the condenser cell, which is mainly composed of three parts. Two cuboids with the angle of 59.4° represent the finned-tube bundles. Each column of cells shares a steam pipe. The axial flow fan is simplified into a round surface. The ACC platform and lateral double-layered deflectors are demonstrated in Fig. 2(a). The two ACCs are next to each other and each ACC contains 56 (7×8) condenser cells, so there are a total of 112 cells in the model, forming a 7-row, 16-column rectangular array. Fig. 2(b) shows the location of the deflectors in *xoy* plane that the upper edges of the two layers of deflectors are at the diameter connections of periphery and secondary periphery fans respectively. By intercepting the *xoz* plane through the center of the fourth row of ACCs, the geometric parameters of different deflectors are displayed in Fig. 2(c) to 2(e), with the first and second columns illustrated. The deflectors are simplified as faces without thickness and next to the bottom of the steel structure. The vertical deflectors are parallel to the *z*-axis and the inclined deflectors are at an angle of 45° [25] to the negative direction of the *x*-axis. The width of all deflectors is 2 m. In this work, "I" represents the inclined deflectors and "V" represents vertical deflectors. Three types of deflectors are named as VV, IV and II respectively, with the first letter representing the outer deflectors and the second letter standing for the inner ones. As shown in Fig. 3, the computational domain is 2400 m×2400 m×720 m, which is large enough to meet the requirements of calculation accuracy.

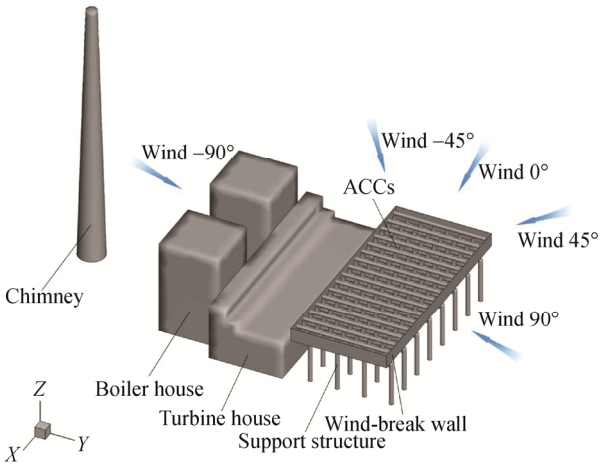

(a) Direct dry cooling power plant and wind directions

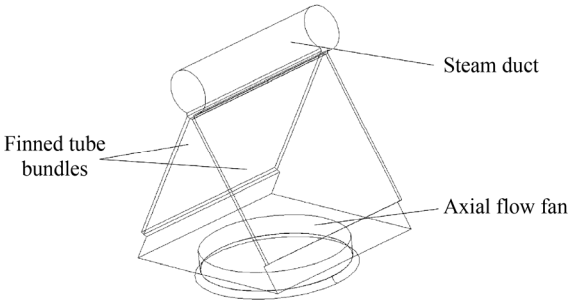

(b) A-frame condenser unit

Fig. 1 Layout of representative 2×660 MW direct dry cooling power plant

2.2 Mathematical models

The steady state Navier-Stokes equation with the following expression is used to govern the air flow and heat transfer for the ACCs:

$$\nabla\cdot\left(\rho\vec{u}\varphi-\Gamma_{\varphi}\nabla\varphi\right)=S_{\varphi}+S'_{\varphi} \tag{1}$$

where φ is the dependent variable and represents different meanings in various equations, such as 1, u, c_pt for the continuum, momentum and energy equations. The realizable k-ε model is applied and φ stands for k and ε in the turbulence equations. Γ_{φ} is the coefficient of diffusion. S_{φ} and S_{φ}' both represent the source term, but the latter is only added to the zone of the finned tube bundles, with the momentum sink S_{m}' in the momentum equation and energy source term S_{e}' in the energy equation as follows:

$$S'_{\mathrm{m}}=-\frac{\Delta p_j}{L_j} \tag{2}$$

$$S'_{\mathrm{e}}=\frac{q_j}{L_j} \tag{3}$$

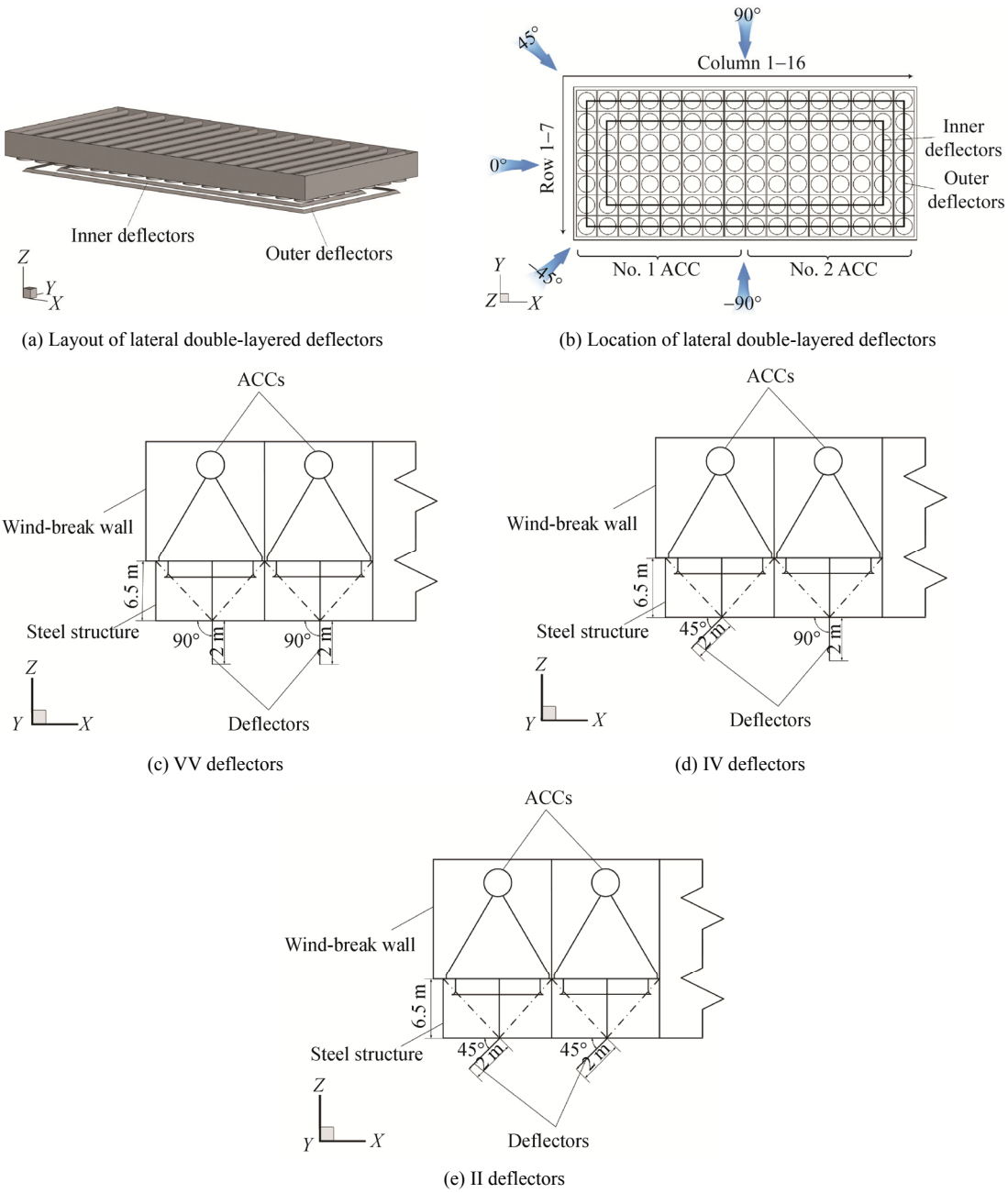

(a) Layout of lateral double-layered deflectors

(b) Location of lateral double-layered deflectors

(c) VV deflectors

(d) IV deflectors

(e) II deflectors

Fig. 2 Deflectors and ACCs

where Δp_j stands for the pressure drop along the flow direction and L_j is the length of flat finned tube bundles. q_j represents heat flux. They are all three-dimensional and j=1, 2, 3 for the three directions respectively.

Steam flows unidirectionally in the finned tube bundle, and the temperature of the steam can be considered to be constant during the condensation process. Therefore, the radiator model is used to calculate the heat transfer between cooling air and finned tube bundles in this study. The pressure drop Δp of cooling air through the finned tube bundles is assumed to be proportional to the face velocity u_f as follows [26]:

$$\Delta p = k_L \frac{1}{2} \rho u_f^2 \tag{4}$$

where k_L stands for the loss coefficient. ρ represents the density of air. The relationship between k_L and u_f is described by the following expression:

$$k_L = \sum_{n=1}^{N} r_n u_f^{n-1} \tag{5}$$

where r_n is the polynomial coefficients. Taking N equal to 5, the values of the polynomial coefficient are r_1=100.81, r_2=–121.07, r_3=78.13, r_4=–23.96, r_5=2.77, which are obtained from the flow experimental results of finned

tube bundles.

The following formula is used to calculate the heat flux q between the tubes and cooling air [27]:

$$q = h\left(t_{\text{wall}} - t_{\text{a}}\right) \tag{6}$$

The above formula can be transformed into the following form for the radiator model to calculate the heat flux:

$$q = h'\left(t_{\text{wall}} - t_{\text{a2}}\right) = h'\left(t_{\text{s}} - t_{\text{a2}}\right) \tag{7}$$

where t_{a2} refers to the outlet air temperature; t_{s} represents the steam condensation temperature and equals t_{wall} approximately. The convective heat transfer coefficient h' is obtained empirically with the following form:

$$h' = \sum_{n=1}^{N} h_n u_{\text{f}}^{n-1} \tag{8}$$

where N is set 3; the values of the polynomial coefficient h_n are h_1 =3015.5, h_2 =386.27, h_3 = –11.976, which are derived from the results of heat transfer experiments.

The three-dimensional real fan is dealt with a fan surface. The pressure rise is a polynomial associated with the axial velocity u_z as follows [28, 29]:

$$\Delta p = \sum_{n=1}^{N} f_n u_z^{n-1} \tag{9}$$

where f_n is the polynomial coefficient and its values refer to Ref. [13].

In order to accurately characterize the fan, the tangential velocity is taken into account in the fan model, so that the cooling air can spiral up. The empirical formula used to calculate the tangential velocity u_θ is as follows [29]:

$$u_\theta = \sum_{n=-1}^{N} g_n r^n \tag{10}$$

where N is set to 5. Detailed data for the polynomial coefficient g_n come from Ref. [13].

The boundary conditions for two typical cases, no wind and the wind direction of 45°, are given in Fig. 3. Under the windless condition, as shown in Fig. 3(a), the pressure inlet boundaries are set for the four sides of the calculation domain and the top is set as the pressure outlet boundary. When the wind blows from the 45° direction, the top can be set as symmetry, as shown in Fig. 3(b). The two faces through which the ambient wind passes firstly are regarded as the velocity inlet while the two downstream faces are outflow. The wind speed u_z varies with the height z as follows [30]:

$$u_z = u_{\text{ref}}\left(\frac{z}{10}\right)^{0.2} \tag{11}$$

In this formula, 10 m is considered as the reference height and u_{ref} stands for the reference wind speed. The ambient temperature is set to 290.15 K according to the rated operating parameters of the power plant.

Since the turbine back pressure reflects the cooling capacity of ACCs directly and is related to the efficiency of power plant, the final back pressure of all cases needs to be achieved by iteration method. The flow rate of exhaust steam is fixed during iterative procedure. For

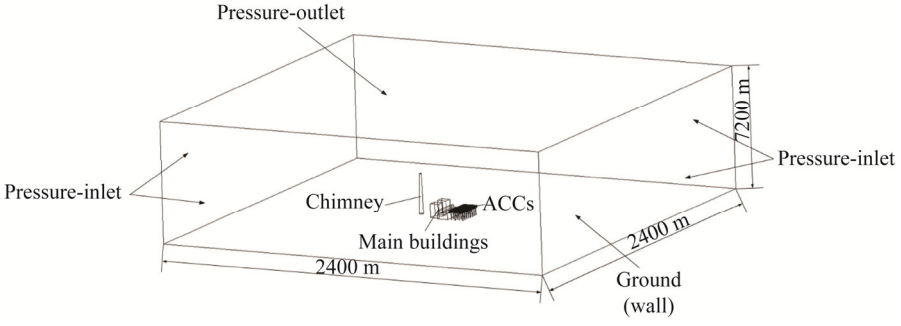

(a) Windless condition

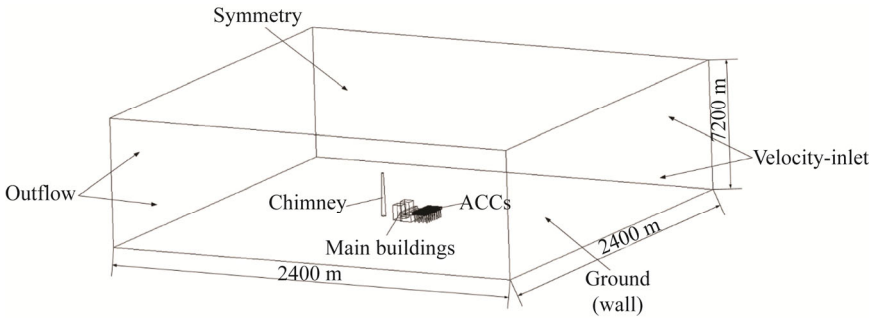

(b) Wind direction of 45°

Fig. 3 Computational domain and boundary conditions

each case, an initial temperature is given to the radiator surface at the beginning of the iteration. This temperature is equal to the condensation temperature and corresponds to a specific back pressure, so the enthalpy of saturated water can be determined. Then the heat rejection of exhaust steam Φ is obtained by the following formula:

$$\Phi = m_{\mathrm{s}}\left(h_{\mathrm{s}} - h_{\mathrm{wa}}\right) \tag{12}$$

where m_{s} represents the flow rate. h_{s} and h_{wa} are the enthalpies of exhaust steam and saturated water respectively. The iteration is finished when the following equation is satisfied:

$$\left|\frac{\Phi - \Phi'}{\Phi}\right| \times 100\% < 0.25\% \tag{13}$$

where Φ' is the air cooling capacity, which can be obtained by CFD simulation.

2.3 Mesh independence and experimental validation

In order to facilitate the meshing, the model is divided into several parts. Two types of grids, tetrahedral unstructured grids and hexahedral structured grids, are adopted for different blocks of the computational domain. The former ones are used for the complex central block, which contains all the buildings and facilities of the power plant. The latter ones are used in other blocks. The farther away from the center, the sparser the grids are, so that the high computational accuracy can be satisfied at the cost of less computational resources.

To verify the independence of the grids, the total grid numbers of 2 310 748, 3 052 216 and 3 855 109 for conventional air-cooled condensers are adopted named as Mesh 1, 2 and 3 respectively. As listed in Table 1, the contrast results of the three different grids show that there are small differences among them under various wind conditions, especially Mesh 2 and 3, so it is feasible to adopt the grid number of 3 052 216. The final grid numbers of ACCs with air deflectors are employed ranging from 3 000 000 to 3 500 000.

Table 1 Mesh independence test results

Parameter		Mesh 1 and 2/ %	Mesh 2 and 3/ %
Mass flow rate difference of ACCs	0 m/s	2.36	0.22
	4 m/s	3.07	0.29
	12 m/s	4.12	0.38
Maximum mass flow rate difference of single fan	0 m/s	2.95	0.31
	4 m/s	3.52	0.40
	12 m/s	4.71	0.46

In order to verify the reliability of numerical simulation, a spot experiment was performed [23] and the difference between the experimental and simulated data is acceptable. In addition, a scaled model experiment was carried out [31]. The performance parameters from the experimental data and numerical simulation results were obtained under the same conditions. The experiment results illustrate that the relative errors of temperatures, mass flow rates and heat rejections in all cases are within acceptable limits and the maximum is 10.57%. Both of them prove that the computational model and approaches are reliable to predict the performances of ACCs.

In order to ensure the reliability of the simulation results of the 2×660 MW direct dry cooling system, the same model and methods as the aforementioned numerical simulations are adopted.

3. Results and Discussion

3.1 Flow and temperature fields

The differences between the deflectors are compared by showing the changes in the temperature, pressure and flow fields. Besides, the variations of the mass flow rates of the fans are more intuitive. As illustrative cases, the thermo-flow characteristics at the wind speed of 12 m/s in three wind directions, 90°, 0° and –90°, will be discussed.

3.1.1 Wind direction of 90°

Fig. 4 gives the temperature distributions of cooling air entering the fans. In the absence of air deflectors, the air temperatures of Row 1 fans are much higher than others, as shown in Fig. 4(a). The increases in the inlet air temperatures of Row 1 and Row 2 fans are obvious while others are close to ambient temperature. It means that the unfavorable influence of wind in this direction is mainly owing to the performance degradation of the fans in the first two rows on the windward side.

Compared to the original ACCs, the inlet air temperatures of ACCs with three different kinds of deflectors have been greatly improved. As shown in Fig. 4(b)–Fig. 4(d), the inlet temperatures of Row 1 and Row 2 fans decrease remarkably, especially for the former ones. The temperatures of Row 2 fans almost reach the ambient temperature except for the ACCs with VV deflectors. Furthermore, the inlet temperature improvements of the IV and II deflectors are almost the same, which are both better than the VV deflectors.

The pressure contours and streamlines of the first three upwind ACCs at the *yoz* plane of Column 9 are given in Fig. 5. It can be seen that a large area with negative pressure is formed at the inlets of the Row 1 and Row 2 fans due to the strong wind. For the ACCs without deflectors shown in Fig. 5(a), the whole inlet area of Row 1 fan and most of the inlet area of Row 2 fan are under negative pressure. The reverse flow for the upwind fan is serious and most of hot air flows from Row 1 condenser cell into Row 2 condenser cell because of the low

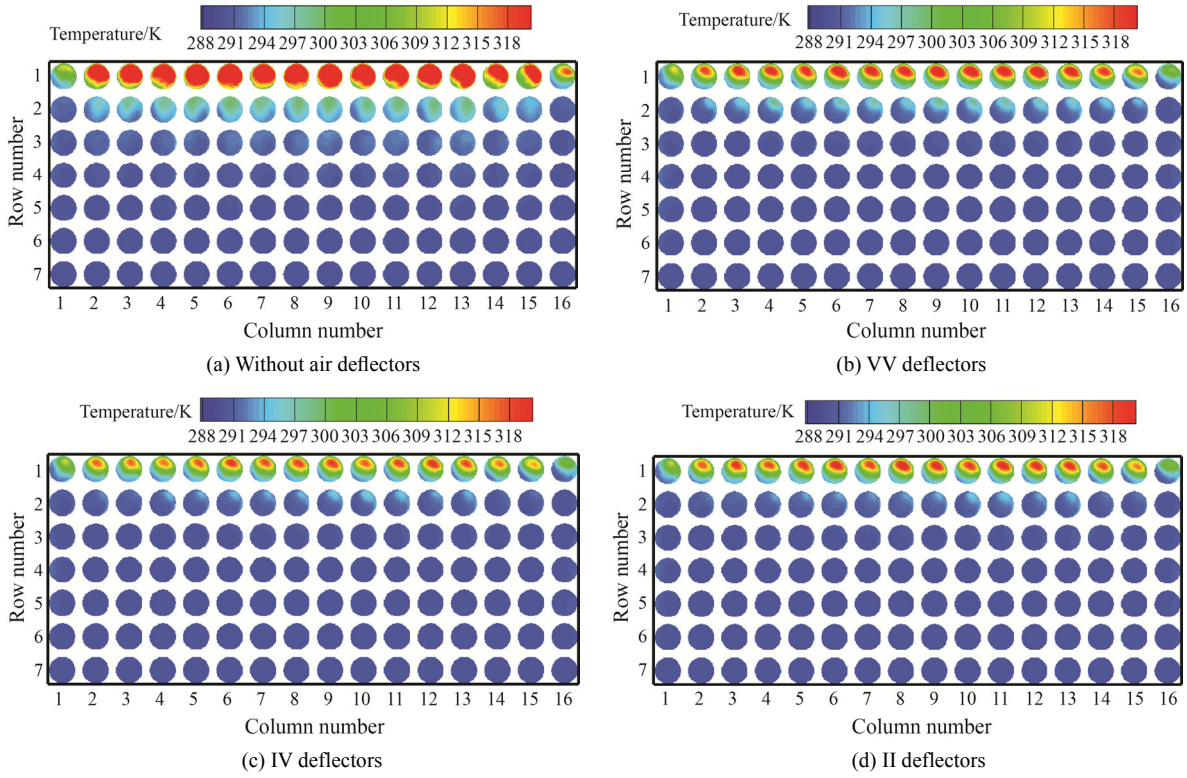

Fig. 4 Inlet air temperatures for different deflectors at wind speed of 12 m/s in 90° wind direction

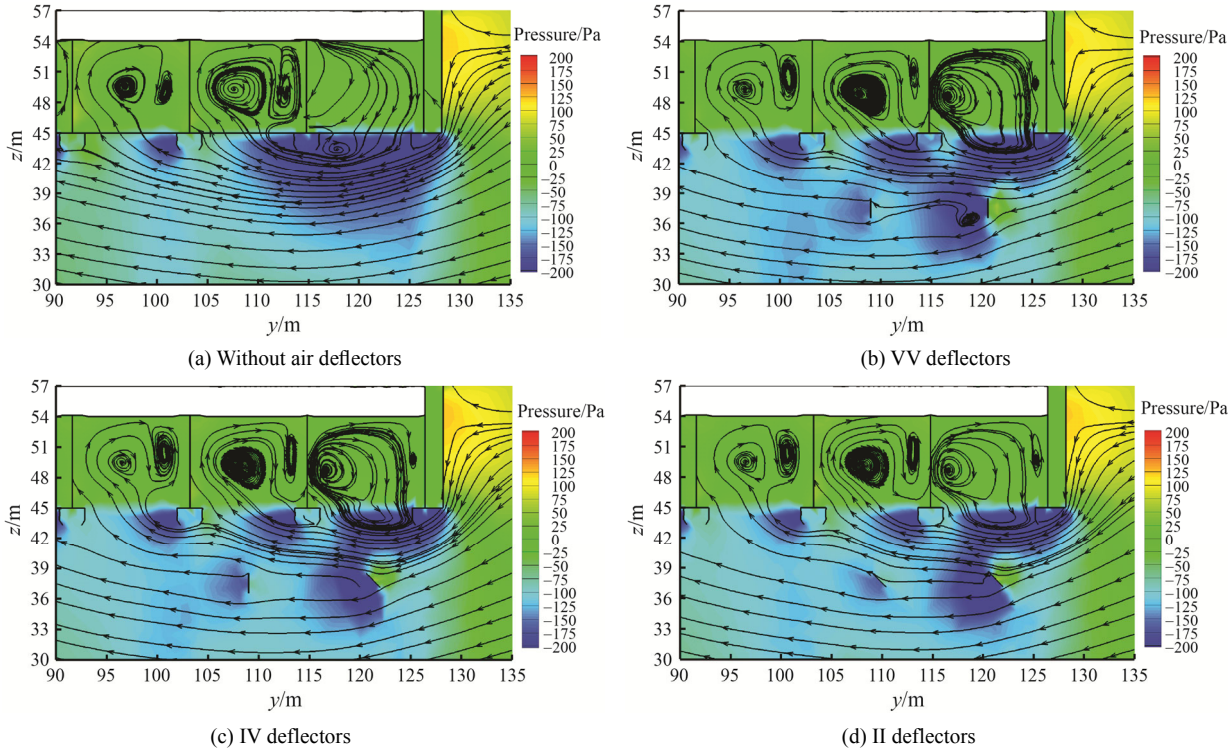

Fig. 5 Static pressures and streamlines of three rows of fans on the windward side in Column 9 at wind speed of 12 m/s in wind direction of 90°

pressure, resulting in the decreases of the flow rates of cooling air sucked by fans and increases of inlet air temperatures of fans in Row 1 and Row 2, which are confirmed in Fig. 4(a). With the deflectors, the negative pressure areas under Row 1 and Row 2 fans are divided into disconnected parts owing to the guiding effects and

become much smaller, which are shown in Fig. 5(b)–Fig. 5(d). The reverse flow is alleviated and little hot air flows from cell 1 to cell 2, leading to the reduced inlet air temperature, which is consistent with Fig. 4. Unfortunately, the negative pressure zone under Row 3 fan is slightly increased in all cases with deflectors.

Fig. 6 presents the comparison of total mass flow rates of fans in each row. The results show that the mass flow rates of Row 1 are negative without deflectors. The mass flow rates of downstream fans increase gradually. With the deflectors, the mass flow rates of Row 1 fans become positive and the increments are 2174, 2486 and 2354 kg/s for the VV, IV and II deflectors respectively. Besides, the mass flow rates of Row 2 fans increase slightly for the ACCs with IV and II deflectors while the opposite result is presented for the ACCs with VV deflectors. In addition, the mass flow rates of Row 3, Row 4 and Row 7 fans are reduced for the ACCs with deflectors. The mass flow rates of cooling air in Row 5 and Row 6 increase for the ACCs with deflectors, which are consistent with Fig. 5. It shows that the IV and II deflectors are more beneficial to the cooling capacity of ACCs.

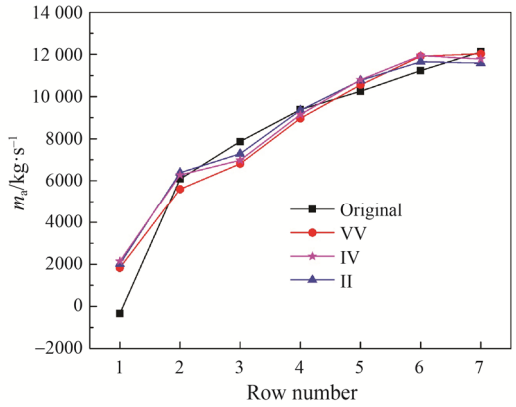

Fig. 6 Mass flow rates at wind speed of 12 m/s in wind direction of 90°

3.1.2 Wind direction of 0°

Fig. 7 shows the temperature distributions of cooling air at the inlet of fans. The inlet air temperatures of windward fans of ACCs without deflectors are much higher than downstream fans under the influence of the wind as shown in Fig. 7(a), with the high temperature more than 320 K. The inlet temperatures of downstream bilateral fans also significantly increase due to the severe hot air recirculation flows [13], which are clearer on the side near the main buildings. For other fans in the middle, the inlet temperatures are hardly affected by the wind along the wind direction, which are equal to the ambient temperature. The inlet temperatures of windward fans are significantly reduced with the deflectors, which are shown in Fig. 7(b)–Fig. 7(d). Especially in Fig. 7(c) and Fig. 7(d), the red high temperature zones have

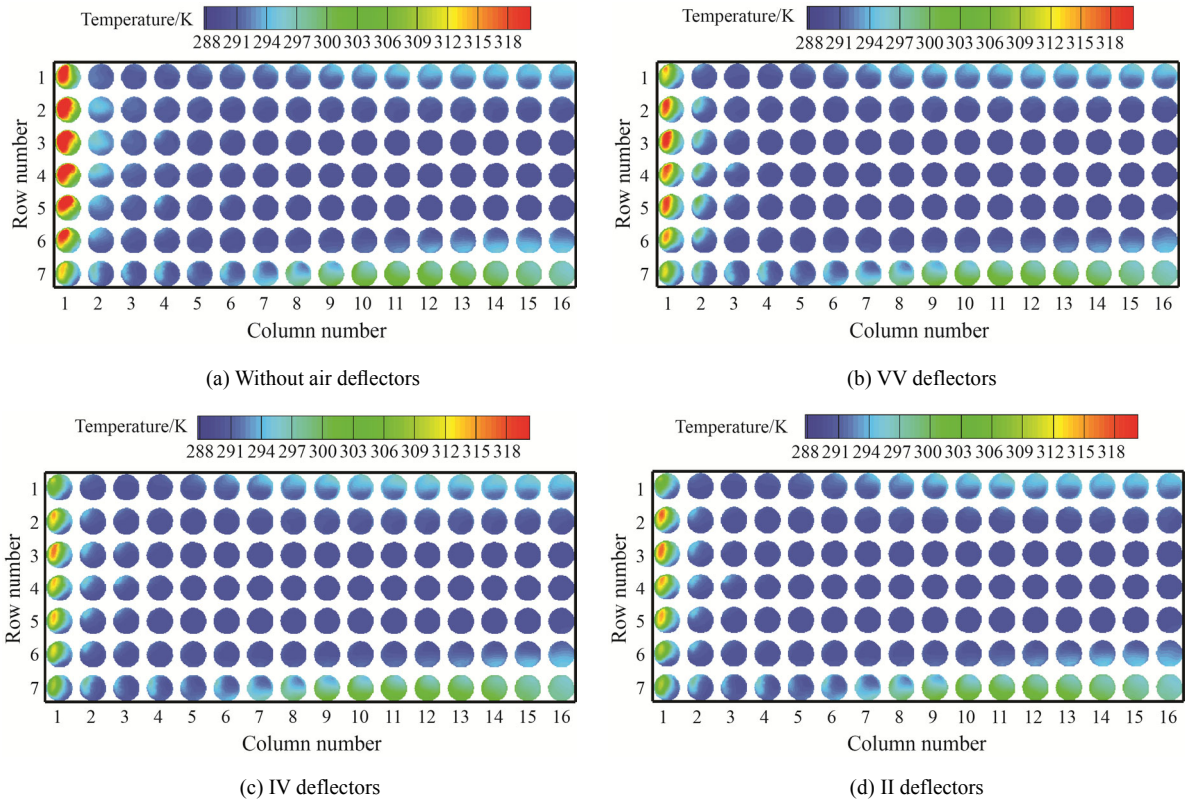

(a) Without air deflectors

(b) VV deflectors

(c) IV deflectors

(d) II deflectors

Fig. 7 Inlet air temperatures for different deflectors at wind speed of 12 m/s in wind direction of 0°

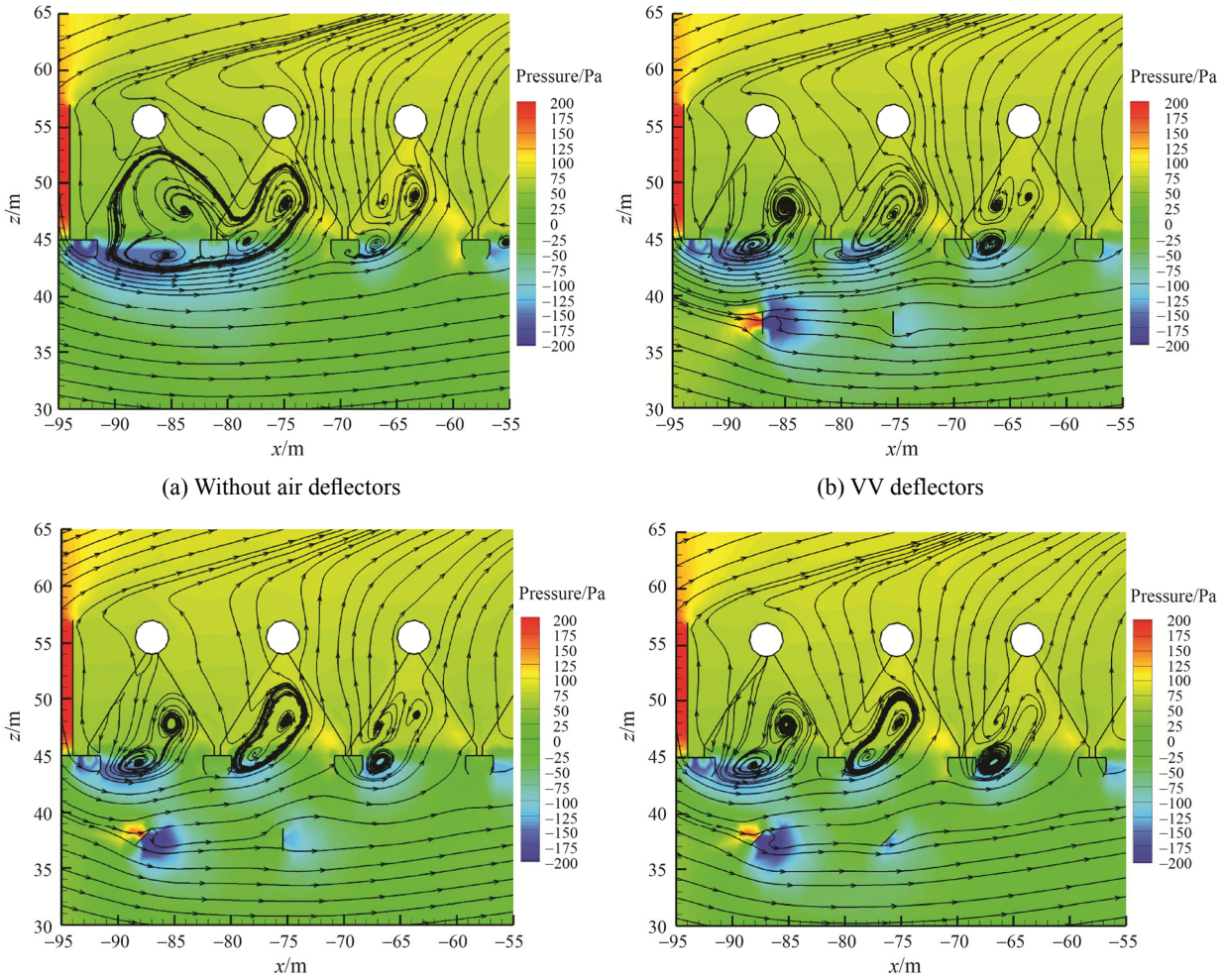

(a) Without air deflectors

(b) VV deflectors

(c) IV deflectors

(d) II deflectors

Fig. 8 Static pressures and streamlines of windward ACCs in Row 4 at wind speed of 12 m/s in wind direction of 0°

disappeared with the presence of IV or II deflectors. But the deflectors have little effects on downstream fans.

The middle row is selected to analyze the local pressure distributions and air streamlines, as shown in Fig. 8. Fig. 8(a) shows the case without deflectors. The negative pressure areas of windward fans are smaller and discontinuous compared to Fig. 7(a). Much hot air circulates between Column 1 and Column 2 condenser cells without the deflectors due to low pressure areas induced by the wind, which severely lowers the cooling capacities of the windward condenser cells due to reduced flow rates and increased inlet temperatures of cooling air. Thanks to the existence of the deflectors, the cooling air is directed upward after flowing through them and the pressure at the inlet of the windward fans increases obviously, as shown in Fig. 8(b)–8(d). The low pressure areas become much smaller and the air recirculation flows between condenser cells are disturbed, which are more clear for the ACCs with IV and II deflectors in Fig. 8(c) and Fig. 8(d).

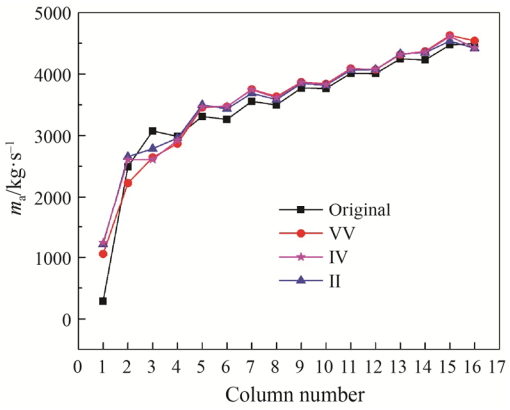

Fig. 9 Mass flow rates at wind speed of 12 m/s in wind direction of 0°

Fig. 9 displays the total mass flow rates of fans in each column. The mass flow rates of Column 1 fans for the ACCs without deflectors are almost close to zero and increase along the wind direction. With VV deflectors, the increment in flow rates of Column 1 fans is 774 kg/s

while the flow rate reductions of the next three columns of fans can be observed. But for the ACCs with IV and II deflectors, the air flow rates of the first two columns of fans increase significantly while the third and fourth columns of fans decrease. Particularly, the increments of mass flow rates of fans in Column 1 are the largest with the values of 956 and 932 kg/s respectively. The main reason may be the changes of the pressure field, as shown in Fig. 8. The increases in the negative pressure zones reduce the flow rates of cooling air entering the corresponding fans for the ACCs with deflectors. Besides, the mass flow rates of downstream columns are enhanced when the deflectors are presented except for the last column.

3.1.3 Wind direction of –90°

Fig. 10 displays the inlet cooling air temperature contours of axial flow fans. The temperature varies widely and basically presents symmetric. In this wind direction, the inlet air temperatures of most of fans are affected by the ambient wind and the highest temperature appears in the bilateral fans. The temperatures of the fans near the main buildings also rise clearly. When the wind blows from the main buildings towards the air-cooled platform, the obstruction of the main building causes vortices near the upwind ACCs, which deteriorate the cooling capacity of ACCs greatly [32]. By comparing with Fig. 10(a), it can be found from Fig. 10(b) to Fig. 10(d) that the temperatures of bilateral fans for the ACCs with IV and II deflectors are lower while the improvements of the temperatures of fans in the middle areas for the ACCs with VV and IV deflectors are more conspicuous.

Fig. 11 shows the streamlines and pressure distributions at the *yoz* plane in Column 14. It can be seen that the negative pressure zones mainly exist at the inlet of the first windward condenser cell, which are different from the aforementioned cases. Due to the main buildings, the cooling air flows into the axial flow fans with a large deflection angle. A big swirl is formed at the inlet of the first fan. As shown in Fig. 11(a), a portion of the reverse air flows into the second fan, which seriously deteriorates the cooling capacity of the first two windward condenser cells for the original ACCs. Thanks to the deflectors, the low pressure areas get reduced and the swirls become much smaller, which are shown in Fig. 11(b)–Fig. 11(d).

The total mass flow rates of fans in each row are shown in Fig. 12. Compared with previous two directions, the difference in air flow rates gets more obvious. For ACCs with VV deflectors, the mass flow rates decrease in Row 4, 5 and 6 and increase in other rows compared

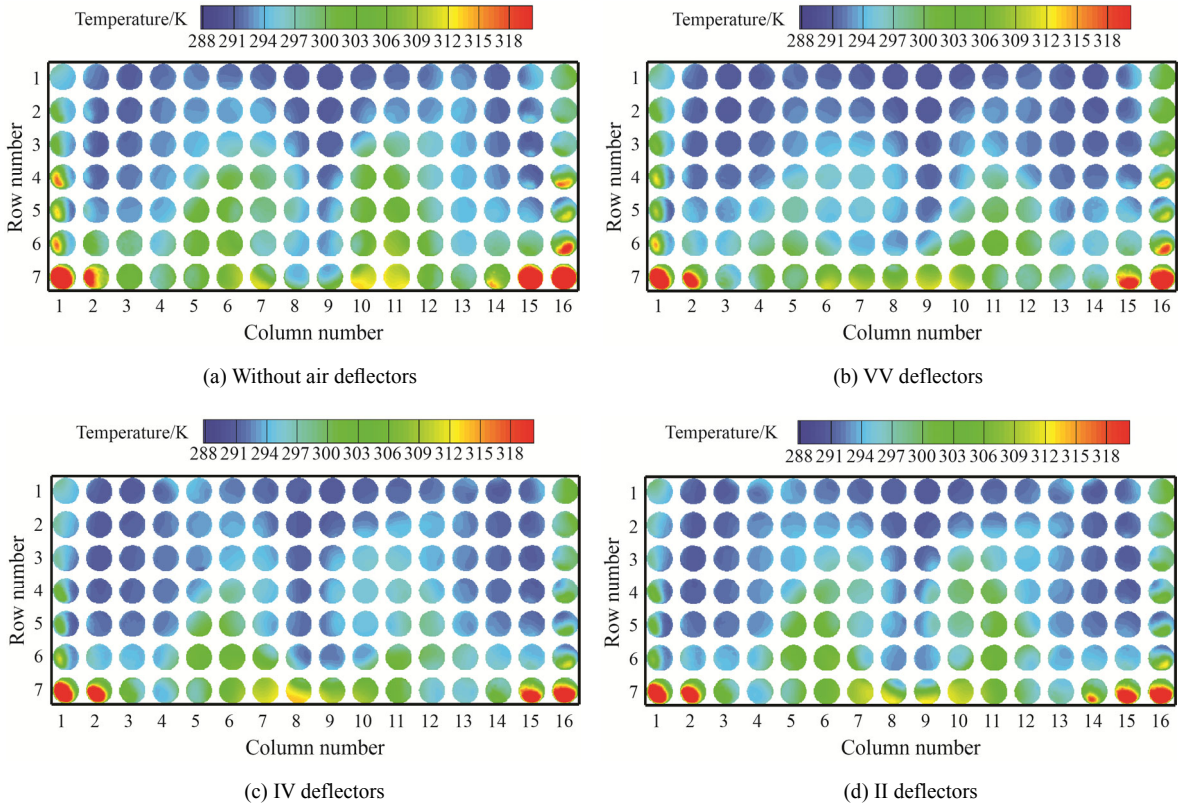

Fig. 10 Inlet air temperatures for different deflectors at wind speed of 12 m/s in wind direction of –90°

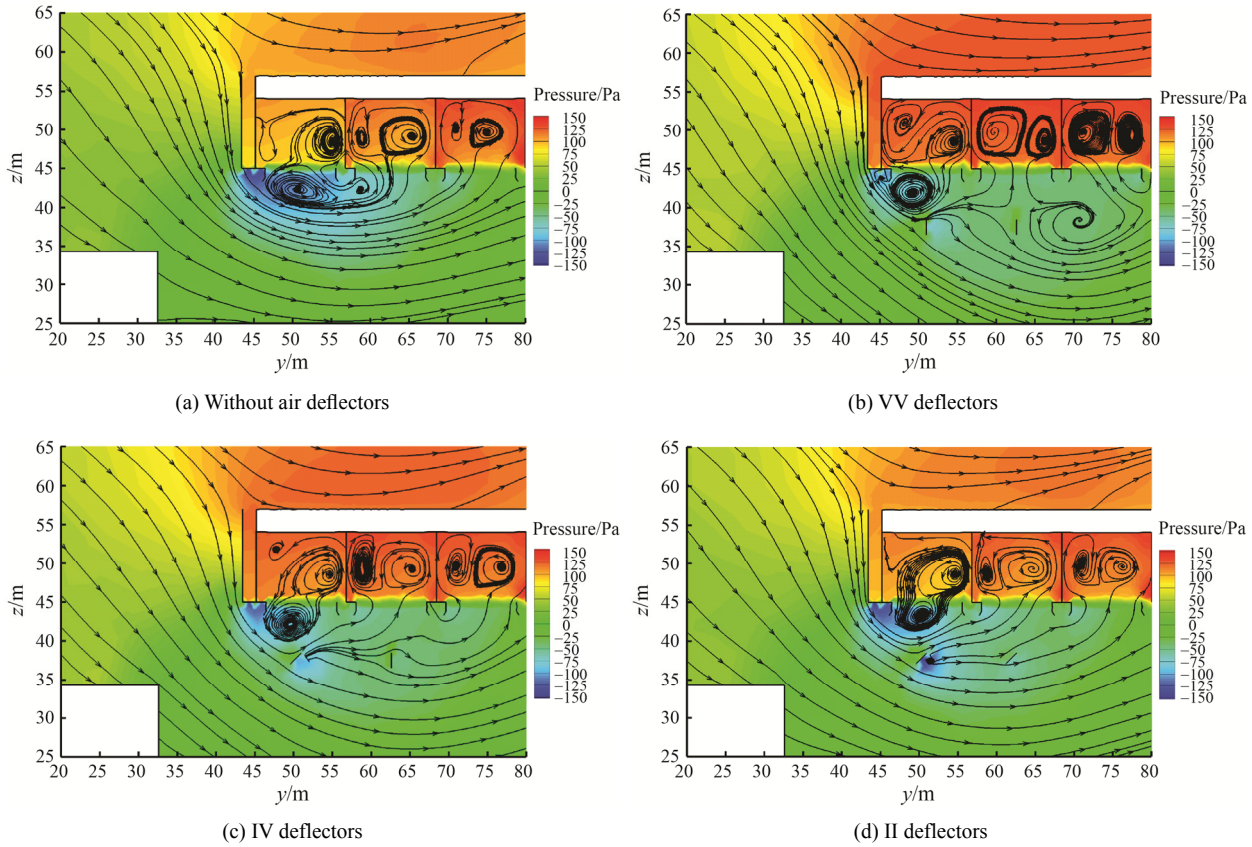

Fig. 11 Static pressures and streamlines of windward ACCs in Column 14 at wind speed of 12 m/s in wind direction of –90°

with the original case. The reduction in flow rates of fans only occurs in the fifth row (the third row on the windward side) for ACCs with IV deflectors. For ACCs with II deflectors, the flow rates of fans have increased in each row. In conclusion, the effects of deflectors IV and II are much better than deflector VV.

3.2 Thermo-flow performances

Under the windless condition, the results are listed in Table 2, which can be seen that the deflectors are beneficial to the performance of ACCs.

The total mass flow rates and back pressures of turbine for the ACCs without and with deflectors are presented and analyzed in five wind directions at two different wind speeds.

Fig. 13(a) shows the results at the wind speed of 4 m/s. The total mass flow rates of ACCs in the wind direction of 0° are significantly greater, showing that the effects of ambient wind in this direction are smaller at low wind speeds. The lowest mass flow rates appear in the wind direction of –90°. The mass flow rates are bigger in the presence of deflectors except for the ACCs with II deflectors in the wind direction of 0°. With IV deflectors, the improvements of total mass flow rates are most conspicuous in all wind directions, which are 3.00%,

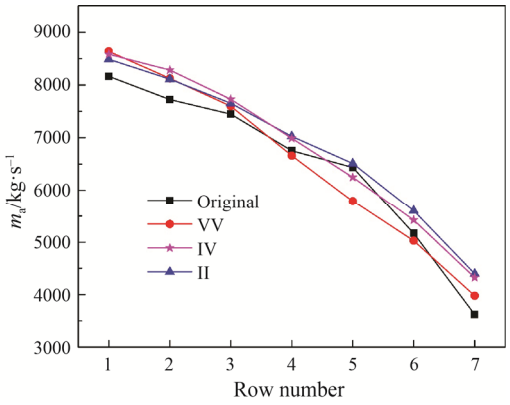

Fig. 12 Total mass flow rates for fans in each row at wind speed of 12 m/s in wind direction of –90°

Table 2 Total mass flow rates and turbine back pressures under windless condition

	m_a/kg·s^{-1}	P_B/kPa
ACCs without deflectors	74 227	16.02
ACCs with VV deflectors	74 482	15.87
ACCs with IV deflectors	74 569	15.87
ACCs with II deflectors	74 482	15.94

2.78%, 0.68%, 1.53% and 1.20% in five wind directions respectively. At the wind speed of 12 m/s, the mass flow rates of cooling air in the wind direction of 90° are the biggest and all types of deflectors are beneficial, as shown in Fig. 13(b). The mass flow rates of ACCs with IV deflectors are superior to others except in the wind direction of –90°, with the improvements of 5.66%, 6.96%, 3.15%, 5.34% and 4.23% in five wind directions respectively. It can be concluded that the effects of deflectors are more pronounced at high wind speeds by comparing Fig. 13(a) and Fig. 13(b).

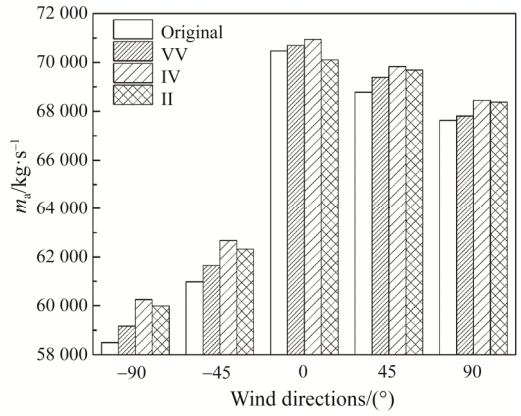

(a) Wind speed of 4 m/s

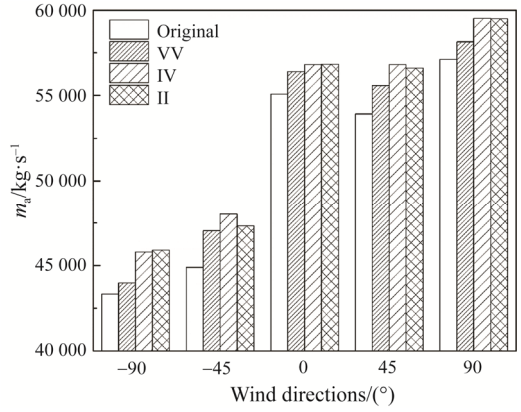

(b) Wind speed of 12 m/s

Fig. 13 Total mass flow rates in five wind directions at wind speeds of 4 m/s and 12 m/s

According to the results of turbine back pressure obtained by iteration, a dimensionless parameter R_p is proposed with the following form to accurately evaluate the influences of deflectors:

$$R_p = \frac{p_{B,o} - p_{B,d}}{p_{B,o}} \times 100\% \tag{14}$$

where $p_{B,o}$ and $p_{B,d}$ represent the turbine back pressures for the original ACCs and ACCs with deflectors respectively.

Ignoring the steam pressure loss from the turbine to condenser, the turbine back pressure p_B can be calculated from the condensation temperature t_s as follows [33]:

$$p_B = 0.009\ 81\left(\frac{t_s + 100}{57.66}\right)^{7.46} \tag{15}$$

Fig. 14 shows the turbine back pressure and dimensionless parameter R_p in different wind directions at two different wind speeds. The back pressure with IV deflectors is the lowest in all cases and the improvement in the wind direction of –45° is the biggest while 0° is the smallest. The improvement effects of the deflectors become greater with the increase of wind speed. For example, the biggest and smallest improvements of ACCs with IV deflectors are 3.71% and 0.47% at the wind speed of 4 m/s while the values are 12.15% and 5.26% at the wind speed of 12 m/s. So the IV deflectors are recommended in practical engineering to improve the cooling capacity of ACCs. The detailed data of mass flow rate and back pressure of all cases are listed in Table 3.

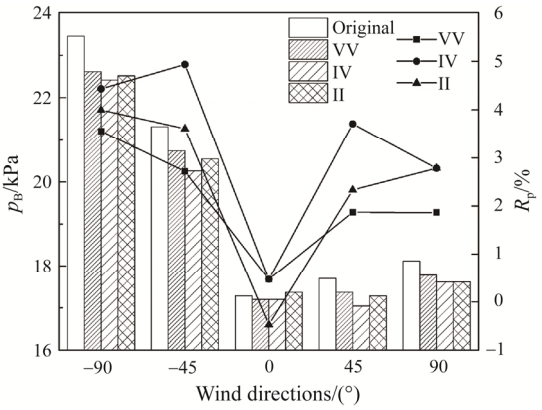

(a) Wind speed of 4 m/s

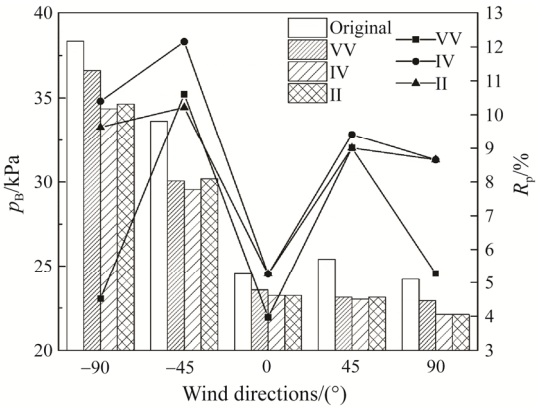

(b) Wind speed of 12 m/s

Fig. 14 Turbine back pressure and dimensionless parameter R_p in five wind directions at two different wind speeds

Table 3 Total mass flow rates of air and back pressures of turbine for ACCs with different deflectors

wind direction	wind speed	deflector cases			
		original	VV	IV	II
		mass flow rate/kg·s^{-1}			
90°	0 m/s	74 227	74 482	74 569	74 482
	4 m/s	67 638	67 814	68 448	68 372
	12 m/s	57 104	58 146	59 518	59 500
45°	4 m/s	68 773	69 381	69 827	69 683
	12 m/s	53 932	55 577	56 813	56 608
0°	4 m/s	70 463	70 688	70 944	70 102
	12 m/s	55 075	56 408	56 809	56 841
–45°	4 m/s	60 973	61 647	62 671	62 314
	12 m/s	44 889	47 033	48 015	47 326
–90°	4 m/s	58 498	59 173	60 253	59 994
	12 m/s	43 331	43 977	45 785	45 900
		back pressure/kPa			
90°	0 m/s	16.02	15.87	15.87	15.94
	4 m/s	18.12	17.78	17.62	17.62
	12 m/s	24.20	22.93	22.11	22.11
45°	4 m/s	17.70	17.37	17.04	17.29
	12 m/s	25.42	23.13	23.03	23.13
0°	4 m/s	17.29	17.20	17.20	17.37
	12 m/s	24.53	23.56	23.24	23.24
–45°	4 m/s	21.31	20.73	20.26	20.54
	12 m/s	33.62	30.06	29.54	30.19
–90°	4 m/s	23.45	22.62	22.41	22.51
	12 m/s	38.34	36.61	34.35	34.64

4. Conclusions

For weakening the adverse wind effects and improving the cooling capacity of ACCs, three kinds of lateral double-layered deflectors installed beneath the ACC platform are proposed. Thanks to the guiding effects, the deflectors are basically beneficial to the thermo-flow characteristics of ACCs by reducing the temperature and increasing the pressure at the inlet of windward fans whether in the absence or present of winds. The results show that the IV deflectors are superior to others especially at high wind speeds. The maximum reduction in turbine back pressure drop is 3.71% at the wind speed of 4 m/s and 12.15% at the wind speed of 12 m/s in the wind directions of –45°. In conclusion, the IV deflectors are preferred in improving the cooling capacity of ACCs, which can be considered for practical application in power plants.

Acknowledgments

The National Natural Science Foundation of China (Grant No. 51476055, 51821004), the National Basic Research Program of China (Grant No. 2015CB251503) and the Fundamental Research Funds for the Central Universities (Grant No. 2018QN036) are gratefully acknowledged for supporting this research.

References

[1] Ge Z., Du X., Yang L., Yang Y., Li Y., Jin Y., Performance monitoring of direct air-cooled power generating unit with infrared thermography. Applied Thermal Engineering, 2011, 31: 418–424.

[2] Duvenhage K., Kröger D.G., The influence of wind on the performance of forced draught air-cooled heat exchangers. Journal of Wind Engineering and Industrial Aerodynamics, 1996, 62: 259–277.

[3] Rooyen J.A.V., Kröger D.G., Performance trends of an air-cooled steam condenser under windy conditions. Journal of Engineering for Gas Turbines & Power, 2008, 130: 277–285.

[4] Owen M., Kröger D.G., Contributors to increased fan inlet temperature at an air-cooled steam condenser. Applied Thermal Engineering, 2013, 50: 1149–1156.

[5] Gu Z., Chen X., Lubitz W., Li Y., Luo W., Wind tunnel simulation of exhaust recirculation in an air-cooling system at a large power plant. International Journal of Thermal Sciences, 2007, 46: 308–317.

[6] Gu Z., Li H., Zhang W., Li Y., Peng J., Wind tunnel simulation on re-circulation of air-cooled condensers of a power plant. Journal of Wind Engineering and Industrial Aerodynamics, 2005, 93: 509–520.

[7] Meyer C.J., Numerical investigation of the effect of inlet flow distortions on forced draught air-cooled heat exchanger performance. Applied Thermal Engineering, 2005, 25: 1634–1649.

[8] Hotchkiss P.J., Meyer C.J., von Backström T.W., Numerical investigation into the effect of cross-flow on the performance of axial flow fans in forced draught air-cooled heat exchangers. Applied Thermal Engineering, 2006, 26: 200–208.

[9] Liu P., Duan H., Zhao W., Numerical investigation of hot air recirculation of air-cooled condensers at a large power plant. Applied Thermal Engineering, 2009, 29: 1927–1934.

[10] Bredell J.R., Kröger D.G., Thiart G.D., Numerical investigation of fan performance in a forced draft air-cooled steam condenser. Applied Thermal Engineering, 2006, 26: 846–852.

[11] Duvenhage K., Vermeulen J.A., Meyer C.J., Kröger D.G., Flow distortions at the fan inlet of forced-draught

air-cooled heat exchangers. Applied Thermal Engineering, 1996, 16: 741–752.

[12] Yang L.J., Du X.Z., Yang Y.P., Space characteristics of the thermal performance for air-cooled condensers at ambient winds. International Journal of Heat and Mass Transfer, 2011, 54: 3109–3119.

[13] Yang L.J., Du X.Z., Yang Y.P., Wind effect on the thermo-flow performances and its decay characteristics for air-cooled condensers in a power plant. International Journal of Thermal Sciences, 2012, 53: 175–187.

[14] Chen L., Yang L., Du X., Yang Y., A novel layout of air-cooled condensers to improve thermo-flow performances. Applied Energy, 2016, 165: 244–259.

[15] Kong Y., Wang W., Huang X., Yang L., Du X., Annularly arranged air-cooled condenser to improve cooling efficiency of natural draft direct dry cooling system. International Journal of Heat and Mass Transfer, 2018, 118: 587–601.

[16] Huang X., Zhang X., Field test and research on heat-transfer performance of plate air-cooled condenser. Procedia Environmental Sciences, 2011, 10: 1148–1153.

[17] Xiao L., Ge Z., Yang L., Du X., Numerical study on performance improvement of air-cooled condenser by water spray cooling. International Journal of Heat and Mass Transfer, 2018, 125: 1028–1042.

[18] Yang L.J., Du X.Z., Yang Y.P., Influences of wind-break wall configurations upon flow and heat transfer characteristics of air-cooled condensers in a power plant. International Journal of Thermal Sciences, 2011, 50: 2050–2061.

[19] Owen M.T.F., Kröger D.G., The effect of screens on air-cooled steam condenser performance under windy conditions. Applied Thermal Engineering, 2010, 30: 2610–2615.

[20] Zhang X., Chen H., Effects of windbreak mesh on thermo-flow characteristics of air-cooled steam condenser under windy conditions. Applied Thermal Engineering, 2015, 85: 21–32.

[21] Zhang X., Wu T., Effects of diffuser orifice plate on the performance of air-cooled steam condenser. Applied Thermal Engineering, 2016, 98: 179–188.

[22] Gu H., Zhe Z., Wang H., Qi C., A numerical study on the effect of roof windbreak structures in an air-cooled system. Applied Thermal Engineering, 2015, 90: 684–693.

[23] Yang L., Du X., Yang Y., Measures against the adverse impact of natural wind on air-cooled condensers in power plant. Science China Technological Sciences, 2010, 53: 1320–1327.

[24] Gao X.F., Zhang C.W., Wei J.J., Yu B., Performance prediction of an improved air-cooled steam condenser with deflector under strong wind. Applied Thermal Engineering, 2010, 30: 2663–2669.

[25] Huang X., Chen L., Kong Y., Yang L., Du X., Effects of geometric structures of air deflectors on thermo-flow performances of air-cooled condenser. International Journal of Heat and Mass Transfer, 2018, 118: 1022–1039.

[26] Chen L., Yang L., Du X., Yang Y., Performance improvement of natural draft dry cooling system by interior and exterior windbreaker configurations. International Journal of Heat and Mass Transfer, 2016, 96: 42–63.

[27] Huang X., Chen L., Yang L., Du X., Yang Y., Cooling performance enhancement of air-cooled condensers by guiding air flow. Energies, 2019, 12: 3503.

[28] Chen L., Yang L., Du X., Yang Y., Novel air-cooled condenser with V-frame cells and induced axial flow fans. International Journal of Heat and Mass Transfer, 2018, 117: 167–182.

[29] ANSYS Inc., Fluent User's Guide, 2012.

[30] Kong Y., Wang W., Zuo Z., Yang L., Du X., Yang Y., Combined air-cooled condenser layout with in line configured finned tube bundles to improve cooling performance. Applied Thermal Engineering, 2019, 154: 505–518.

[31] Kong Y., Wang W., Huang X., Yang L., Du X., Yang Y., Circularly arranged air-cooled condensers to restrain adverse wind effects. Applied Thermal Engineering, 2017, 124: 202–223.

[32] Jin R., Yang X., Yang L., Du X., Yang Y., Square array of air-cooled condensers to improve thermo-flow performances under windy conditions. International Journal of Heat and Mass Transfer, 2018, 127: 717–729.

[33] Yang L.J., Wu X.P., Du X.Z., Yang Y.P., Dimensional characteristics of wind effects on the performance of indirect dry cooling system with vertically arranged heat exchanger bundles. International Journal of Heat and Mass Transfer, 2013, 67: 853–866.